Journal of Magnetism and Magnetic Materials 474 (2019) 570–573

Contents lists available at ScienceDirect

Journal of Magnetism and Magnetic Materials

journal homepage: www.elsevier.com/locate/jmmm

Research articles

Determination of dominating relaxation mechanisms from temperature-dependent Magnetic Particle Spectroscopy measurements

S. Draack*, T. Viereck, F. Nording, K.-J. Janssen, M. Schilling, F. Ludwig

Institute for Electrical Measurement Science and Fundamental Electrical Engineering, Technische Universität Braunschweig, Hans-Sommer-Straße 66, D-38106 Braunschweig, Germany

ARTICLE INFO

Keywords:
Magnetic Particle Spectroscopy
Temperature dependence
Magnetic nanoparticles
Magnetization dynamics
Brownian relaxation
Néel relaxation

ABSTRACT

Magnetic Particle Spectroscopy (MPS) is a characterization method for investigating the nonlinear properties of magnetic nanoparticles (MNP) using magnetic field strengths in the order of a few tens of millitesla. Its exploitation for particle characterization is of high significance for biomedical applications such as Magnetic Particle Imaging (MPI) and magnetic hyperthermia. Since the dynamic characteristics of MNP are influenced by both the Néel and the Brownian relaxation mechanism, harmonic spectra in MPS measurements are directly linked to ambient influences like temperature or viscosity of the surrounding medium. Experimental data of multiparametric measurements helps one to evaluate and validate mathematical models of dynamic particle magnetization. This contribution deals with the investigation of temperature-dependent harmonic spectra of different commercially available single-core and multi-core particle systems. It is shown, that dominating relaxation mechanisms can be determined from temperature-dependent MPS measurements.

1. Introduction

Magnetic Particle Spectroscopy (MPS) was developed as a zero-dimensional measurement method to examine the suitability of magnetic nanoparticles (MNP) for the medical imaging modality Magnetic Particle Imaging (MPI) [1]. MPS and MPI are both based on the same nonlinear dynamic properties of MNP. When excited by an externally applied magnetic field, the resulting higher harmonics of the magnetization processes are very sensitive to small changes of particles' environments. Although MNP are commonly used as tracer materials in medical imaging [2,3] or magnetic hyperthermia approaches, signal generation is still a wide area of research. Often, the dependence of harmonic ratios (e.g. A_5/A_3) is addressed [4] but the complex behavior of higher harmonics or even the total harmonic spectra is neglected, although higher harmonics contain sensitive information and are of particular importance for functional MPI. This contribution deals with the investigation of temperature-dependent harmonic spectra in MPS measurements. Fokker–Planck simulations help to understand the effects of temperature on the measured data and enable one to attribute the dominating dynamic magnetization process. These information are of particular interest for e.g. the evaluation of the suitability of MNP for mobility MPI (mMPI) [5] or magnetic hyperthermia [6].

2. Theory

The cores of magnetic nanoparticles (MNP) with diameter d_c and core volume typically consist of a ferro- or ferrimagnetic material with a specific saturation magnetization M_s. Due to their small sizes, the thermal fluctuations of the particles lead to a zero net magnetization in absence of an externally applied magnetic field. Therefore, the quasi-static magnetization behavior of magnetic nanoparticles is described by the Langevin function

$$M_L(H) = M_s \cdot \left(\coth(\xi) - \frac{1}{\xi} \right), \tag{1}$$

where $\xi = \frac{E_M}{E_T}$ denotes the ratio between magnetic energy $E_M = mB$ and thermal energy $E_T = k_B T$ using the magnetic moment $m = M_s V_c$, the externally applied flux density B, the Boltzmann constant k_B and the temperature T. However, the magnetic response of magnetic nanoparticles in dynamic applications is significantly influenced by magnetization dynamics. Thus, only dynamic models can be used to explain dependencies on physical values. One of the most common approaches to describe such relationships is a numerical model based on the Fokker–Planck equation [7] which describes the cylindrically symmetric time-varying probability density function W of the magnetic moment m. For a symmetry of the magnetic interaction energy with

* Corresponding author.
E-mail address: s.draack@tu-bs.de (S. Draack).

https://doi.org/10.1016/j.jmmm.2018.11.023
Received 22 June 2018; Received in revised form 5 September 2018; Accepted 4 November 2018
Available online 05 November 2018
0304-8853/

respect to a line in direction z and easy axes aligned along the z-axis, the partial differential equation is given by

$$2\tau_0 \frac{\partial W}{\partial t} = \frac{\partial}{\partial x}\left[(1-x^2)\left(\frac{\partial W}{\partial x} - \frac{mB}{k_B T} W - \frac{2KV_c}{k_B T} xW\right)\right]. \quad (2)$$

The Fokker–Planck equation includes an intrinsic field dependence and just requires the field-independent relaxation time τ_0 of the appropriate relaxation process. The influence of the anisotropy energy $E_K = KV_c$ including the anisotropy constant K occurs in the case of Néel relaxation only and must be neglected for Brownian relaxation. The temporal evolution depends on the polar angle θ between the field direction vector z and the direction of the magnetic moment $\vec{m}$, in which x denotes the cosine of θ and can be expressed by the dot product of the field unit direction vector $\vec{z}$ and the reduced magnetic moment vector $\vec{m}_0 = \frac{\vec{m}}{|\vec{m}|}$. The Fokker–Planck equation can be solved by an expansion in terms of Legendre polynomials and results in two different numerically solvable iterative algorithms for both the Brownian and the Néel relaxation process. The coefficients for the Brownian relaxation (FP-B) can be calculated from

$$\frac{da_n}{dt} = \frac{n(n+1)}{2\tau_{B0}} \cdot \left[-a_n + \frac{mB}{k_B T}\left(\frac{a_{n-1}}{2n-1} - \frac{a_{n+1}}{2n+3}\right)\right]. \quad (3)$$

Here, the Brownian zero-field relaxation time $\tau_{B0} = \frac{3\eta V_h}{k_B T}$ including the hydrodynamic volume $V_h = \frac{1}{6}\pi d_h^3$ with the particles' hydrodynamic diameter d_h and the dynamic viscosity η of the medium must be used. The temperature dependence of the dynamic viscosity is described by the Arrhenius–Andrade relation $\eta = \eta_0 \exp\left(\frac{E_A}{E_T}\right)$ including the medium-specific activation energy E_A [8]. For the following simulations, the dynamic viscosity was set to the one of water neglecting the amount of particles due to the small mass percentage. The Néel relaxation algorithm (FP-N) includes another term describing the anisotropy dependence. Furthermore, the field-independent Néel relaxation time $\tau_{N0} = \tau_0 \exp\left(\frac{KV_c}{k_B T}\right)$ must be considered instead of the Brownian zero-field relaxation time. The coefficients for the Néel relaxation are given by

$$\frac{da_n}{dt} = \frac{n(n+1)}{2\tau_{N0}} \cdot \left[-a_n + \frac{mB}{k_B T}\left(\frac{a_{n-1}}{2n-1} - \frac{a_{n+1}}{2n+3}\right) + \frac{2KV_c}{k_B T}\left(\frac{a_{n-2}(n-1)}{(2n-3)(2n-1)} + \frac{a_n}{(2n-1)(2n+3)} - \frac{a_{n+2}(n+2)}{(2n+5)(2n+3)}\right)\right]. \quad (4)$$

The time-dependent magnetization signal

$$M(t) = cM_s V_c \cdot \frac{2}{3} a_1(t) \quad (5)$$

for n particles with the molar particle concentration c, where $[c] = 1/m^3$ can be derived from the first order moment of the Legendre coefficients. Subsequently, a digital lock-in method [9] is used to evaluate the odd higher harmonics of the simulated magnetization signal.

3. Methods & materials

agnetic Particle Spectroscopy (MPS) utilizes a pure sinusoidal excitation signal to force the net magnetic moment of the magnetic nanoparticles into the saturation regime. The change of the magnetization response induces a voltage in a gradiometric detection coil, which is amplified and measured using an analog–digital converter directly connected to a personal computer. A Fourier transform or digital lock-in method of the measured signal leads to a frequency domain representation. Since the excitation signal and therefore the magnetization response is symmetric around zero, the measured signal contains odd higher harmonics only. To be able to better distinguish series of curves, the higher harmonics are typically linked by lines. Our custom-built MPS setup allows temperature-dependent measurements in a wide sample temperature control range from − 20 °C to 120 °C and was first introduced in [10]. Furthermore, different series resonant circuit stages are available to match the inductance of the excitation coil allocating a set of excitation frequencies in the range 100 Hz ≤ f_0 ≤ 25 kHz. Additionally and more trivially, a change of the excitation field amplitude can be used to perform multi-parametric MPS measurements. A differential pick-up coil providing an attenuation of the excitation field of − 70 dB_V enables a measurement of higher harmonics as well as the fundamental frequency generated by the particles. Samples were prepared as undiluted suspensions (iron concentrations $c_{Fe,SHP}$ = 5 mg mL^{-1} and $c_{Fe,synomag}$ = 25 mg mL^{-1}) in ThermoFisher Nunc MaxiSorp™ microtiter vials with an amount of 150 µL each from commercially available stock material for different types of magnetic nanoparticle systems SHP-25 and SHP-30 ordered from Ocean NanoTech (San Diego, California) and synomag®-D from micromod Partikeltechnologie GmbH (Rostock, Germany). Corresponding particle properties, which were determined from AC susceptometry (ACS) measurements by fitting a generalized Debye model [11], were used for the simulations and are summarized in Table 1. In comparison to SHP-30, Ocean NanoTech SHP-25 exhibit a mean core diameter of $d_c \approx 25$ nm and a corresponding hydrodynamic diameter of $d_h \approx 50$ nm.

Table 1
Particle properties of Ocean NanoTech SHP-30 and micromod synomag®-D.

Parameter	SHP-30	synomag®-D
M_s/kA m^{-1}	366	366
d_c/nm	30	20
d_h/nm	57	34
K/kJ/m^3	5.0	5.0

4. Simulation

To be comparable to measurement results, the magnetic field amplitude of the pure sinusoidal excitation signal was set to $H_0 = 25\,\mathrm{mT}/\mu_0$ and the frequency was set to $f_0 = 1$ kHz for the following simulations. All data in this contribution are normalized to M_{max} representing the magnitude maximum value (which is the fundamental's magnitude) for each set in the series of temperature-dependent curves. Furthermore, we concentrate on the magnitude spectra of the magnetization $|M(f)|$ only. The Langevin function explains the nonlinear magnetization curve of isotropic superparamagnetic nanoparticles in a static scenario. The temperature dependence of simulated higher harmonics based on the Langevin function model are plotted in Fig. 1 exemplarily for SHP-30 particle properties. The steepness of the magnetization curve becomes shallower for increasing temperatures. This relationship results in decreasing higher harmonics in the frequency domain representation of the magnetization signal for increasing temperatures. Since MPS excitation typically works in the

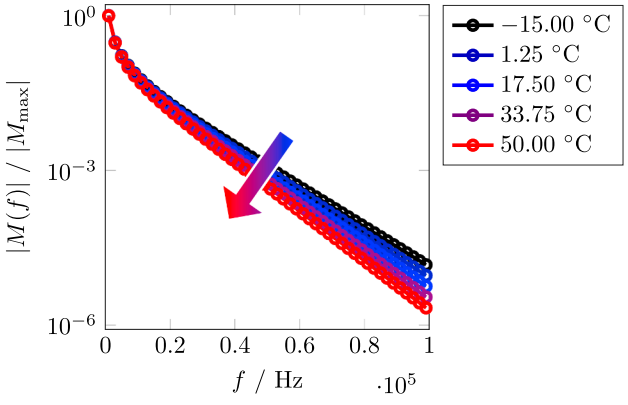

Fig. 1. Temperature dependence of simulated harmonic spectra for Ocean NanoTech SHP-30 based on Langevin function model.

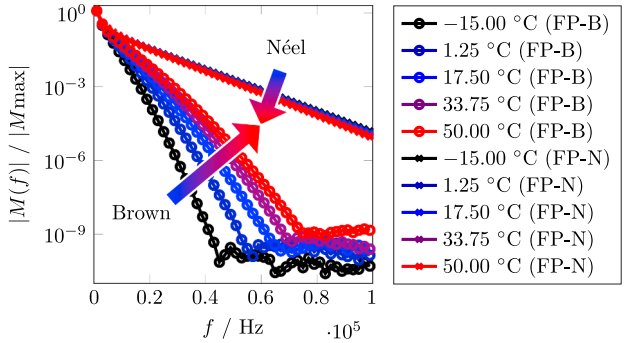

(a) Ocean NanoTech SHP-30 parameters

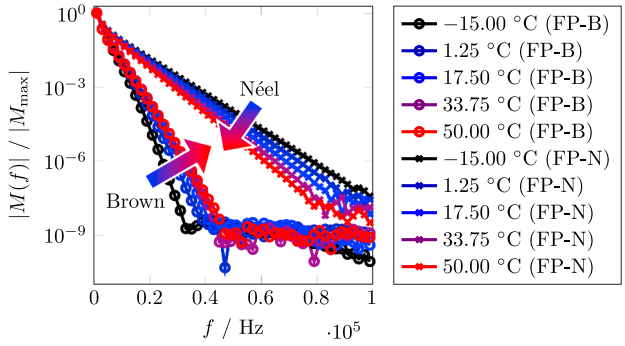

(b) micromod synomag®-D parameters

Fig. 2. Temperature dependence of simulated harmonic spectra for Ocean NanoTech SHP-30 and micromod synomag®-D based on Fokker–Planck equations. Particle parameters are given in Table 1. Arrows indicate the trend of higher harmonics for increasing temperatures.

kilohertz regime, measurement results are – depending on the particle properties – particular sensitive to both dynamic magnetization mechanisms [12,13]. Fig. 2 depicts the temperature dependence of simulated harmonic spectra based on Fokker–Planck equations (3) and (4) implemented in a Python simulation environment exploiting the `lsoda` solver for stiff ordinary differential equations (SODE). As both equations describe a single relaxation mechanism only and do not allow to predict coupled behavior, two temperature-dependent series of curves are shown for each particle system. Simulations were performed for the particle properties given in Table 1 and normalized to the magnitude of the fundamental frequency. As can be seen in Fig. 3b, the Brownian simulation results show a more significant temperature influence than the Néel simulation results for the same range of temperatures. Furthermore, the trend is inverse for both relaxation mechanisms. Néel simulations show a drop of the higher harmonics for increasing temperatures, while the magnitude of the higher harmonics increases for the Brownian simulations. The trend is similar for synomag®-D particle properties as it is shown in Fig. 2, but the temperature influence in the Brownian simulation results is less pronounced, while the temperature dependence for Néel simulations is more distinct. The differences between the two simulations of different particle parameters are due to the size properties. It should be noted, that presented simulation data were generated neglecting particle size distributions. Nevertheless, the simulations represent qualitative trends which will be discussed in comparison with experimental data.

5. Experimental

Experimental MPS magnitude spectra for Ocean NanoTech SHP-30 and micromod synomag®-D are shown in Fig. 3. Measurements were performed for a comparably low excitation frequency of $f_0 = 1$ kHz at

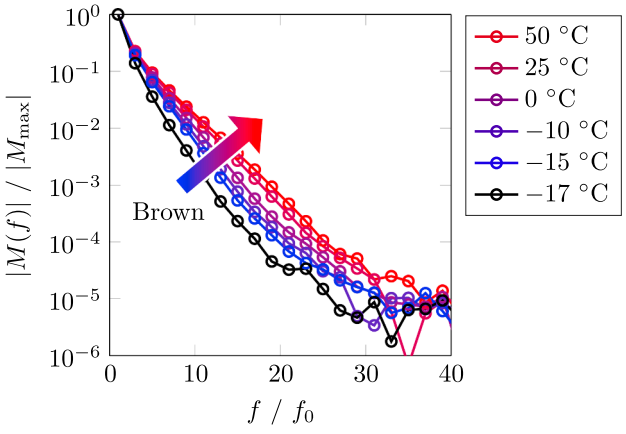

(a) Ocean NanoTech SHP-30

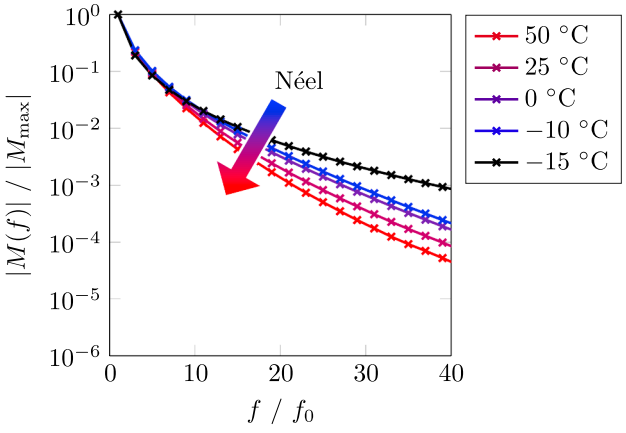

(b) micromod synomag®-D

Fig. 3. Temperature dependence of measured harmonic spectra for Ocean NanoTech SHP-30 and micromod synomag®-D particle suspensions acquired at $f_0 = 1$ kHz and $\mu_0 H = 25$ mT.

an excitation field amplitude $H_0 = 25\ \mathrm{mT}/\mu_0$ to be especially sensitive to Brownian relaxation. For SHP-30 (Fig. 3a), increasing sample temperatures lead to more pronounced higher harmonics. The decay of the higher harmonics is significantly flattened at high temperatures. Compared to the change of the higher harmonics at low temperatures from − 10 °C to − 15 °C, a non-continuous jump of the higher harmonics is observed for the small temperature change of − 2 °C from − 15 °C to − 17 °C which is due to the optically verified phase transition of the particle suspension to ice. The synomag®-D particle suspension shows an opposing temperature-dependent trend of the higher harmonics as can be seen from Fig. 3b. The non-continuous jump of the higher harmonics which is due to the suspension's frozen state is observed at − 15 °C. Further measurements were performed using Ocean NanoTech SHP-25, which exhibit similar magnetic properties as SHP-30. The temperature dependence of the higher harmonics of SHP-25 acquired at $f_0 = 5$ kHz and $H_0 = 25\ \mathrm{mT}/\mu_0$ is shown in Fig. 4. Conspicuously, a crossing of the temperature-dependent series of curves is observed.

6. Discussion

A comparison of experimental with simulated data allows one to link the temperature dependence with the dominating relaxation mechanism as it is already annotated in all figures. Since the magnitudes of the higher harmonics of the single-core particle system SHP-30 increase for increasing temperatures (Fig. 2a), the prevailing dominated

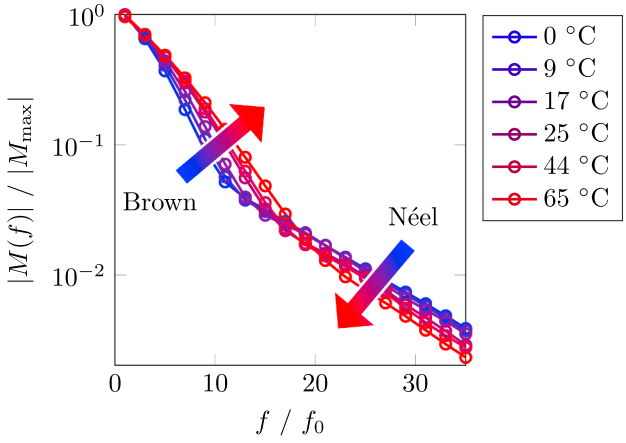

Fig. 4. Temperature dependence of measured harmonic spectra of Ocean NanoTech SHP-25 suspension acquired at $f_0 = 5$ kHz and $\mu_0 H = 25$ mT.

relaxation mechanism can be attributed to the Brownian rotation of particles (Fig. 3b). Measurements of the multi-core particle system synomag®-D show the opposite behavior of the harmonic response (Fig. 2b) which is due to a Néel-dominated relaxation process as corresponding simulations in Fig. 2 indicate. MPS measurements of SHP-25 show a crossing of the temperature-dependent series of curves, which can be traced back to an appearance and coupling of both relaxation mechanisms. While lower odd harmonics exhibit a positive temperature coefficient (the magnitude increases with increasing temperatures), higher odd harmonics possess a negative temperature coefficient (the magnitude decreases with increasing temperatures). Thus, the sample contains a mixture of particles dominated by the Brownian relaxation mechanism and by the Néel relaxation mechanism. Similar sharp bends in the linked curves of higher harmonics are often observed in MPS measurements. Typically, lower harmonics exhibit a steep decay, while higher harmonics feature a shallow decay and minor magnitudes. The temperature-dependent results approve an assignment of both parts to specific relaxation behavior.

7. Conclusion & outlook

Experimental data of temperature-dependent MPS measurements contain sensitive information about dynamic particle magnetization properties. Measurement results were compared to Fokker–Planck simulations to explain physical dependencies. In this case, the acquisition of a set of different temperatures for the same sample enables the conclusion of the dominating relaxation process at a certain excitation frequency and field amplitude due to opposing temperature coefficients of the Brownian and the Néel relaxation mechanism. Furthermore, complex crossings of the temperature-dependent series of curves of SHP-25 can be attributed to superimposing and coupled relaxation mechanisms. To verify the relationships, extended [14] and coupled modeling approaches including core and hydrodynamic size distributions are required, which will be explored in future work.

Acknowledgment

Financial support by the German Research Foundation DFG via Priority Program SPP1681 (VI 892/1-1, LU 800/4-3) is acknowledged.

Appendix A. Supplementary data

Supplementary data associated with this article can be found, in the online version, at https://doi.org/10.1016/j.jmmm.2018.11.023.

References

[1] S. Biederer, Magnet-Partikel-Spektrometer, Springer Vieweg, 2012.
[2] C. Kuhlmann, A.P. Khandhar, R.M. Ferguson, S. Kemp, T. Wawrzik, M. Schilling, K.M. Krishnan, F. Ludwig, Drive-field frequency dependent MPI performance of single-core magnetite nanoparticle tracers, IEEE Trans. Magn. 51 (2014), https://doi.org/10.1109/TMAG.2014.2329772.
[3] F. Ludwig, C. Kuhlmann, T. Wawrzik, J. Dieckhoff, A. Lak, A.P. Kandhar, R.M. Ferguson, S.J. Kemp, K.M. Krishnan, Dynamic magnetic properties of optimized magnetic nanoparticles for Magnetic Particle Imaging, IEEE Trans. Magn. 50 (2014), https://doi.org/10.1109/TMAG.2014.2329504.
[4] N. Löwa, M. Seidel, P. Radon, F. Wiekhorst, Magnetic nanoparticles in different biological environments analyzed by magnetic particle spectroscopy, J. Magn. Magn. Mater. 427 (2017) 133–138, https://doi.org/10.1016/j.jmmm.2018.10.096.
[5] T. Viereck, C. Kuhlmann, S. Draack, M. Schilling, F. Ludwig, Dual-frequency magnetic particle imaging of the Brownian particle contribution, J. Magn. Magn. Mater. 427 (2017) 156–161, https://doi.org/10.1016/j.jmmm.2016.11.003.
[6] M. Javidi, M. Heydari, M.M. Attar, M. Haghpanahi, A. Karimi, M. Navidbakhsh, S. Amanpour, Cylindrical agar gel with fluid flow subjected to an alternating magnetic field during hyperthermia, Int. J. Hyperther. 31 (1) (2014) 33–39, https://doi.org/10.3109/02656736.2014.988661.
[7] R.J. Deissler, Y. Wu, M.A. Martens, Dependence of Brownian and Néel relaxation times on magnetic field strength, Int. J. Med. Phys. Res. Pract. 41 (1) (2014), https://doi.org/10.1118/1.4837216.
[8] V.M. Gutsalyuk, I.S. Guly, Y.B. Mel'nichenko, V.V. Klepko, G.I. Vasil'ev, N.N. Avdeev, Mutual diffusion in aqueous gel solutions, Polym. Int. 33 (1994) 359–365, https://doi.org/10.1002/pi.1994.210330403.
[9] J.M. Masciotti, J.M. Lasker, A.H. Hielscher, Digital lock-in algorithm for biomedical spectroscopy and imaging instruments with multiple modulated sources, 2006 International Conference of the IEEE Engineering in Medicine and Biology Society, IEEE, 2006, , https://doi.org/10.1109/iembs.2006.259303.
[10] S. Draack, T. Viereck, C. Kuhlmann, M. Schilling, F. Ludwig, Temperature-dependent MPS measurements, Int. J. Magn. Part. Imag. 3 (1) (2017), https://doi.org/10.18416/ijmpi.2017.1703018.
[11] F. Ludwig, C. Balceris, C. Jonasson, C. Johansson, Analysis of AC susceptibility spectra for the characterization of magnetic nanoparticles, IEEE Trans. Magn. 53 (11) (2017) 1–4, https://doi.org/10.1109/tmag.2017.2693420.
[12] T. Wawrzik, C. Kuhlmann, H. Remmer, N. Gehrke, A. Briel, M. Schilling, F. Ludwig, Effect of Brownian relaxation in frequency-dependent magnetic particle spectroscopy measurements, in: 2013 International Workshop on Magnetic Particle Imaging (IWMPI), 2013, p. 1.https://doi.org/10.1016/j.jmmm.2018.11.023.
[13] J. Dieckhoff, D. Eberbeck, M. Schilling, F. Ludwig, Magnetic-field dependence of Brownian and Néel relaxation times, J. Appl. Phys. 119 (2016), https://doi.org/10.1063/1.4940724.
[14] T. Wawrzik, T. Yoshida, M. Schilling, F. Ludwig, Debye-based frequency-domain magnetization model for magnetic nanoparticles in Magnetic Particle Spectroscopy, IEEE Trans. Magn. 51 (2) (2014), https://doi.org/10.1109/TMAG.2014.2332371.